DOI: 10.7860/JCDR/2023/64549.18613

Original Article

Anatomy Section

p16INK4a and γ-H2AX as Biomarkers of Senescence in Skin Tissue: A Cadaveric Cross-sectional Study at a Tertiary Care Centre in Punjab, India

RICHA GUPTA[1], ANJALI AGGARWAL[2], TULIKA GUPTA[3], CHIMAN KUMARI[4]

ABSTRACT

Introduction: Baseline expression of p16INK4a characterises cellular senescence. Similarly, the measurement of γ-Gamma-H2AX (γ-H2AX) foci levels in cells provides a reliable method for quantification of Deoxyribonucleic Acid (DNA) damage.

Aim: To explore the role of p16INK4a and γ-H2AX as biomarkers of senescence in skin tissue.

Materials and Methods: This was a cross-sectional study conducted in the Department of Anatomy, PGIMER, Chandigarh, Punjab, India from June 2022 to January 2023. Skin tissue was obtained from 30 cadavers, aged 20-90 years, from the anterior abdominal wall. The time duration of sample collection after death varied from six hours to 12 hours. Samples were divided into two groups: Group-I <30 years and Group-II >70 years, with n=15 in each group. The relative change in the expression pattern of p16INK4a and γH2AX markers, as well as the microstructure of the skin (thickness of epidermis and dermis, distribution of collagen I/II/III fibres, architecture of sebaceous glands), were statistically analysed using an unpaired t-test.

Results: Intense staining was observed with p16INK4a in Group-II, showing positivity in 60.75% of the cells, while Group-I depicted a weak staining pattern (15%). On immunostaining with γ-H2AX, only Group-II cells showed intense positivity (45%). Significant differences were observed in the epidermal and dermal thickness: Group-I (165.5267±37.73 μm; 2394.6±874.13 μm); Group-II (54.6±22.79 μm; 566.67±242.23 μm), and collagen Type-II/III fibres were found predominantly in aging skin tissue.

Conclusion: The present study provides comprehensive data regarding age-associated changes between p16INK4a, γ-H2AX, and skin microstructure, which result in decreased repair and regenerative capacity of skin tissue and various age-related skin diseases.

Keywords: Aging, Deoxyribonucleic acid damage, Histology, Regenerative, Skin diseases

INTRODUCTION

Senescence is a progressive degenerative process occurring in various tissues of the body in response to metabolic alterations, reactive oxygen species, and various other factors. Due to these changes, cells enter into permanent cell cycle arrest and start secreting various kinds of Senescence-associated Secretory Phenotypes (SASP) [1-4]. The International Cell Senescence Association has advocated the use of a combination of different markers and expression of SASP factors to correctly identify senescent cells [3]. P16INK4a is one of the typical markers accepted as a marker of ageing and senescence. It was originally identified as a cell cycle inhibitor and is intensely investigated as a marker of senescence [5-7]. Furthermore, immunolabelling with γ-H2AX provides direct visualisation and quantitative measurement of double-stranded DNA breaks as fluorescent nuclear foci. Therefore, the γ-H2AX assay has been widely applied to a variety of cell types and tissues to correlate its expression pattern with DNA damage and repair [8,9]. Based on the available literature, it can be hypothesised that with advanced ageing, p16INK4a and γ-H2AX expression might show variability in skin tissue of various age groups. The discovery of various senolytic therapies to prevent age-related degenerative changes in the skin and treat various age-related skin disorders requires detailed knowledge about the factors and senescent pathways involved in the ageing process of skin tissue [5]. Although many studies have investigated the expression pattern of p16INK4a or γ-H2AX in various other tissues [5-8], to date, there is no comprehensive study exploring the combined changes in the expression pattern of these two markers as well as microstructural changes in skin tissue with advancing age. Therefore, the current study aimed to study the role of p16INK4a and gamma-H2AX as biomarkers of senescence in skin tissue. This knowledge might pave the way for various interesting therapeutic or diagnostic options to prevent age-related skin disorders among humans.

MATERIALS AND METHODS

This was a cross-sectional study conducted in the Department of Anatomy at PGIMER, Chandigarh, Punjab, India from June 2022 to January 2023. Skin tissue was obtained from 30 cadavers aged 20-90 years. The time duration of sample collection after death varied from 6 hours to 12 hours. The site of sample collection was the anterior abdominal wall. The study was conducted in accordance with Helsinki guidelines, and informed written consent was obtained from each donor/kin or relatives of donors for the use of their body for research purposes at the time of body donation.

Inclusion criteria: Tissue was collected from grossly normal-looking cadavers without any signs of trauma or surgical intervention.

Exclusion criteria: Cadavers with macerated skin or a medical history of diabetes, cancer, or any other chronic disease were excluded from the study.

Sample size: A total of 30 tissue samples were selected for the study. The tissue samples were arranged into two age groups: Group-I <30 years and Group-II >70 years (with n=15 in each group).

Study Procedure

Fresh skin tissue samples were obtained from the cadavers before the embalming procedure. The tissue samples were fixed in a 10% neutral buffered formalin solution for approximately 24 hours, followed by washing with tap water for 5-6 hours. Then, the tissue was soaked in 70% alcohol overnight. Subsequently, the tissue

was treated with ascending grades of alcohol (70%, 80%, 90%, absolute alcohol-I, absolute alcohol-II, and absolute alcohol-III) for 1 hour each, followed by treatment with three changes of toluene (Toluene I, Toluene II, Toluene III) for one hour each. The tissue was then impregnated in paraffin wax by treating it with three changes of wax (wax-1, wax-2, wax-3) for 1.5 hours each, after which block formation was done.

Immunohistochemical staining: Formalin-fixed skin tissues were embedded in paraffin and sectioned to a thickness of 4-5 μm thickness, placed on polylysine-coated slides, and processed for Immunohistochemistry (IHC). The slides were placed in a 56-60°C oven for 15 minutes. Afterwards, dewaxing in xylene was performed by treating the slides with three changes of xylene for five minutes each to remove paraffin wax. This was followed by rehydration in decreasing concentrations of alcohol: two changes of absolute alcohol for three minutes each, followed by 90% alcohol for three minutes, and 70% and 50% alcohol for three minutes each. The slides were then placed in Phosphate Buffered Saline (PBS) solution until further steps. For the blocking step, the sections were incubated for 20 minutes at room temperature in a mixture of PBS solution and 0.3% H_2O_2. After washing with PBS solution, the samples were retrieved using boiled Citrate Buffer Solution (CBS) in a microwave for 12 minutes. After another wash with PBS, the sections were incubated for 16-18 hours at 4°C with the primary antibody anti-CDKN2A/p16INK4a antibody (DCS50.1; ab16123, Abcam, Boston, MA) at a 1/5000 dilution. They were then washed three times with PBS for five minutes each and incubated for two hours at room temperature with the secondary antibody Goat Anti-mouse IgG H&L (Alexa Fluor® 488) (ab150113; Abcam, Boston, MA). The sections were rinsed in PBS and developed in a solution of 0.025% 3,3'-diaminobenzidine and 0.003% H2O2 under microscopic control at room temperature to visualise peroxidase activity. The sections were then rinsed in distilled water, counterstained with Mayer's haematoxylin, and mounted using Dibutylphthalate Polystyrene Xylene (DPX). Control for the staining procedure included the omission of the secondary antibody from the reaction sequence. Light microscopic slides were photographed using an Olympus BX50 microscope (Olympus, Tokyo, Japan) and analysed with the help of software (ProgRes CapturePro 2.9.01) [Table/Fig-1a-e].

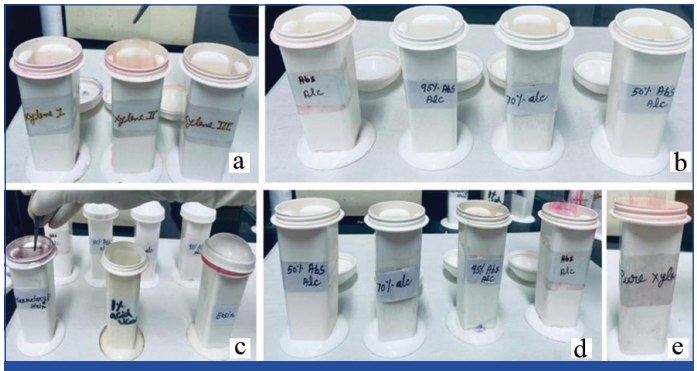

[Table/Fig-1]: Steps of Haematoxylin and Eosin staining: (a) Tissue slides were given three changes of xylene (2 minutes each); (b) Further, slides were treated with descending grades of alcohol-absolute alcohol; 95% alcohol; 70% alcohol, 50% alcohol (2 minutes each); (c) Then, slides were rinsed in running tap water (2 minutes), stained with Cole's haematoxylin solution for 15-20 minutes, followed by differentiation in 1% acid alcohol (mixture of 70% alcohol and 1-2 drops of HCl) and bluing under tap water for 15 minutes. Then slides were counterstained with 1% Eosin solution for 30 seconds; (d) After previous step, sections were treated with ascending grades of alcohol (50%, 70%, 95%, absolute alcohol); (e) followed by clearing in pure xylene solution.

The percentage of positive cells was calculated using Image J software. The total number of cells as well as the number of positive cells were counted using the software in 10 high-power fields (10 hpf). The percentage of positive cells was then calculated as follows:

Percentage of positive cells=(Total number of positive cells per 10 hpf/ Total number of cells per 10 hpf)×100

H scoring [10] was used to assess differences in IHC staining in the observed tissues. This was done by evaluating the percentage of positively stained cells and calculating the intensity of staining in the individual slides under a light microscope using established criteria. The H-Score was calculated using the following formula:

H-Score=(1xN′1′)+(2xN′2′)+(3xN′3′)

Here, N corresponds to the percentage of positive cells, where 1 represents mildly positive, 2 represents moderately positive, and 3 represents strongly positive staining. The cells in which clear IHC staining was observed at 40X, 20X, and 10X magnification were considered mildly, moderately, and strongly positive, respectively.

Immunofluorescence staining: Formalin-fixed skin tissues were embedded in paraffin and sectioned to a thickness of 4 μm. The tissue was placed on polylysine-coated slides. After dewaxing in xylene and rehydration in decreasing concentrations of alcohol, the sections were boiled in Citrate Buffer Solution (CBS). The sections were then incubated with Anti-γH2AX antibody {ab195188-Recombinant Alexa Fluor® 488 antibody; EP854 (2)Y}. Finally, the sections were mounted with 4′,6-Diamidino-2-Phenylindole (DAPI). γH2AX positive cells were studied and analysed using a Nikon E600 epifluorescent microscope (Nikon, Düsseldorf, Germany). The microscope was equipped for the excitation and emission wavelengths of Alexa Fluor 488 and DAPI. Digital images for qualitative and quantitative image analyses were analysed using imaging software (Image J software). With the help of Image J software, the number of γ-H2AX positive cells was counted per 10 high-power fields (10 hpf). The percentage of positive cells was then calculated as follows:

Percentage of positive cells=(Total number of positive cells per 10 hpf/ Total number of cells per 10 hpf)×100

Haematoxylin and Eosin (H&E) staining [Table/Fig-1]: Formalin-fixed skin tissues were embedded in paraffin and sectioned to a thickness of 4-5 μm. The tissue was placed on glass slides. Paraffin was cleared from the samples by three changes of xylene (2 minutes each). To hydrate the samples, the slides were treated with absolute alcohol, 95% alcohol, 70% alcohol, and 50% alcohol (2 minutes each). Then, the slides were rinsed in running tap water (2 minutes), stained with Cole's haematoxylin solution (for nuclear staining) for 15-20 minutes, followed by differentiation in 1% acid alcohol (a mixture of 70% alcohol and 1-2 drops of HCl) and bluing under tap water for 15 minutes. The slides were then counterstained with 1% eosin solution (to stain cytoplasm and extracellular matrix) for 30 seconds. After this, the tissue sections were dehydrated by treating the slides with ascending grades of alcohol (50%, 70%, 95%, Absolute alcohol), followed by clearing in pure xylene solution [Table/Fig-1]. Finally, cover slips were mounted on slides using DPX, and the slides were viewed under a light microscope. Epidermal and dermal thickness were measured digitally in micrometres with the help of software (ProgRes CapturePro 2.9.01) on an Olympus BX53 microscope (Olympus, Tokyo, Japan). Epidermal thickness was considered from the outer surface of the stratum corneum to the dermal papilla and epidermal rete ridges, respectively. For dermal thickness, measurements were taken from the dermoepidermal junction to the dermis-fat junction. For each specimen, the average value was considered as the final value. Images were captured with an Olympus BX53 microscope (Olympus, Tokyo, Japan) and analysed with the help of software (ProgRes CapturePro 2.9.01). The architecture of the sebaceous gland was studied by observing the staining intensity of nuclei and cell cytoplasm.

Picrosirius red staining: Formalin-fixed skin tissues were embedded in paraffin and sectioned to a thickness of 4 μm. The tissue was placed on glass slides. The paraffin sections were then dewaxed and hydrated. The nuclei were stained with Wiegert's haematoxylin for eight minutes, and the slides were washed for 10 minutes in running tap water. Further, the sections were stained with Picrosirius red for

one hour and then washed with two changes of acidified water. Water was removed from the slides by vigorous shaking, and the sections were dehydrated in three changes of 100% ethanol, cleared in xylene, and mounted in a resinous medium.

On Picrosirius red staining, changes in the distribution of collagen Type-I, Type-II, and Type-III fibres were determined among both age groups by observing the slides under an Olympus BX53 microscope (Olympus, Tokyo, Japan) with the help of a polariser. The slides were digitally photographed using software (ProgRes CapturePro 2.9.01). Type-I collagen fibres mostly showed red or reddish-yellow birefringence, while Type-II and Type-III collagen fibres showed green birefringence under a polarised microscope.

Images were captured with an Olympus BX53 microscope (Olympus, Tokyo, Japan) and analysed with the help of software (ProgRes CapturePro 2.9.01).

STATISTICAL ANALYSIS

The entire dataset was entered into a sheet in an excel workbook (Microsoft Office Excel; version 2007, Microsoft Corporation, USA) and analysed. Descriptive statistics, including the mean, standard deviation, and range, were evaluated using GraphPad Prism Version 8.0.1 (244) software. The staining intensity, as well as the number of γH2AX and p16INK4a positive keratinocytes, was evaluated. The total number of positive cells was counted in 10 high-power fields (40X), and then their mean was calculated. The difference in epidermal and dermal thickness between Group-I and Group-II was calculated using an unpaired t-test. All the above findings were considered statistically significant if the p-value was <0.05.

RESULTS

Expression of anti-p16Ink4a: Intense staining of p16INK4a, a senescence marker, was observed in Group-II. H scoring was used to assess IHC staining differences in the observed tissues. In Group-I, p16Ink4a positive cells were significantly fewer and mostly distributed among the basal layer of skin biopsies from young donors. In Group-I, only 15% of the cells showed positivity for p16INK4a (305/2032 cells per 10 hpf). The IHC scoring intensity or H scoring for p16INK4a positive cells in Group-I was 36 in the stratum basale layer. With increasing age, epidermal cells underwent senescent changes, and the number of p16Ink4a positive cells increased. In Group-II, almost 60.75% (765/1259 cells per 10 hpf) of the cells were found to be p16Ink4a positive and were distributed among the stratum spinosum, in addition to the stratum basale layer of the epidermis. H scoring for p16INK4a positive cells in Group-II was 72 in the stratum basale and 165 in the stratum spinosum [Table/Fig-2a,b].

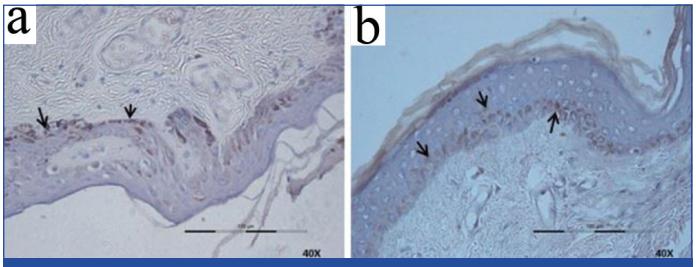

[Table/Fig-2]: Immunohistochemical analysis of p16INK4a staining in skin tissue: Photomicrograph (a) revealed Group-I showing positive expression of p16INK4a in stratum basale layer (arrows); Photomicrographs (b) revealed Group-II showing positive expression of p16INK4a in stratum basale and stratum spinosum (arrows) with significantly large number of positive cells showing intense staining pattern (Original magnification 40X with scale bar 100 μm).

Expression of γH2AX: In the current study, it was observed that the expression of γH2AX positive keratinocytes in the epidermis showed positivity only in the advanced age group. Additionally, the relative expression of γH2AX positive keratinocytes was analysed in different epidermal layers. The overall expression of γH2AX positive cells in the epidermis was observed only in Group-II (45%). 34% of γH2AX positive cells were observed in the stratum basale and 11% in the stratum spinosum. On high-power field (40X), puncta (DNA damage foci within nuclei) were visible within cells, indicating the presence of fragmented DNA [Table/Fig-3a-f]. Increased expression of γH2AX positive cells was observed in the stratum basale and stratum spinosum layers (45%), out of which 25% of nuclei showed the presence of puncta or intranuclear foci (2±.2).

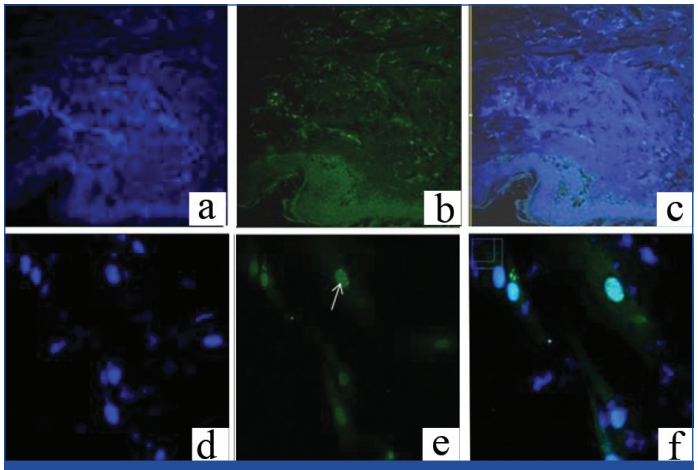

[Table/Fig-3]: Skin tissue was immunostained with γ-H2AX antibody and counterstained with DAPI: the picture was taken by epifluorescence microscopy (a,d) Photograph of DAPI fluorescence associated with DNA content (blue); (b,e) The γ-H2AX positive cells are mainly localised in the stratum basale and stratum spinosum layer in Group-II (>70 years) and appear in green colour; White arrow in Fig 3e showing punctum, reflecting DNA damage foci; (c,f) Merged staining pattern showing staining of cells with γ-H2AX (green) and counterstaining of nuclei with DAPI (blue). Photomicrographs (a,b,c) were taken in low power (10X); Photomicrographs (d,e,f) were taken in high power (40X).

Haematoxylin and Eosin staining: In Group-I, the mean thickness of the epidermis, extending from the surface of the epidermis to the dermal papilla, was observed to be 32.42±17.09 μm, ranging from 16.36-74.2 μm [Table/Fig-4a]. In Group-II, the minimum mean thickness was observed to be 16.64±5.03 μm, ranging from 10.34-29.66 μm [Table/Fig-4b]. The p-value was observed to be 0.0016, indicating a statistically significant difference in the thickness of the epidermis between both groups. Similarly, the mean thickness of the epidermis, extending from the surface of the epidermis to the epidermal ridges, in Group-I was 165.53±37.73 μm, ranging from 113.2-216.4 μm [Table/Fig-4c], while in Group-II, it was observed to be 54.59±22.79 μm, ranging from 16.22-82.39 μm [Table/Fig-4d]. The p-value was observed to be <0.0001, showing a statistically highly significant difference in the thickness of the epidermis between the elderly population and the young population.

In Group-I, all the layers of the epidermis could be clearly demarcated. The stratum spinosum consisted of 4 to 5 layers in most cases, and the stratum granulosum layer was well-differentiated. Basal layer cells were either columnar or short cuboidal, with elongated nuclei [Table/Fig-4c]. However, in Group-II [Table/Fig-4d], different layers of the epidermis could not be well differentiated. The stratum granulosum was not well demarcated, and the stratum spinosum consisted of only two to three layers of cells in most cases (80%). Furthermore, the cells showed signs of degeneration, such as nuclear lysis and nuclear fragmentation. The cell boundaries of different layers appeared to be dissolved, making it difficult to demarcate different layers of the skin among the older age population [Table/Fig-4d].

In Group-I, the stratum corneum layer was well-defined and closely apposed to the rest of the layers of the epidermis, but in a few cases, separation of the stratum corneum from the rest of the epidermal layers was observed. In Group-I, the papillary layer of the dermis was thinner compared to the reticular layer, and it had papillary protrusions on the epidermis side, forming a corrugated and firm link with the epidermis. The mean thickness of the dermis in Group-I was observed to be 2394.6±874.13 μm, ranging from 1059-3831 μm [Table/Fig-5,6a]. In Group-II, the thickness of the dermis was observed to be 449.54±242.23 μm, ranging from 224.2-1088 μm [Table/Fig-6b]. This

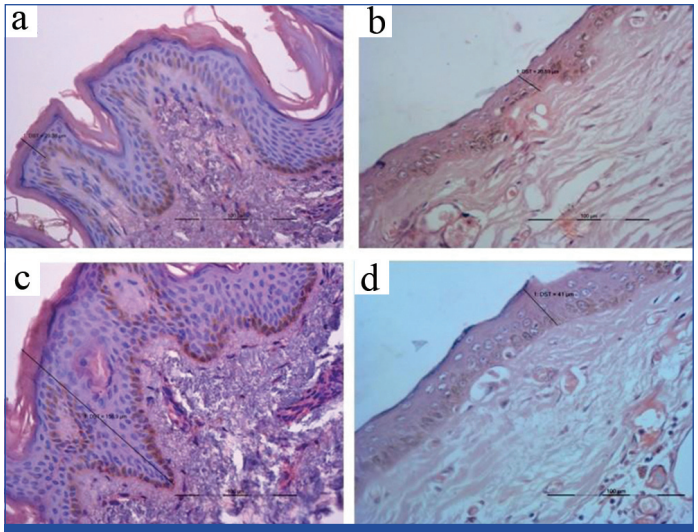

[Table/Fig-4]: Human skin tissue showing thickness of epidermis in both groups: Group-I (<30 years); Group-II (>70 years). a,b) showing thickness of epidermis from the surface of epidermis upto dermal papilla in Group-I and Group-II, respectively; c,d) showing thickness of epidermis extending from the surface of epidermis upto epidermal ridges in Group-I and Group-II, respectively (H&E stain, original magnification 40X with scale bar 100 μm).

difference was found to be statistically significant (p-value 0.0088). In Group-I, the dermal-epidermal ridges were well-defined, and a large number of dermal papillae could be observed. However, in Group-II, the depth of the dermal papillae was decreased, and in most cases, there was flattening of the dermal-epidermal ridges.

Epidermal and dermal thickness (in μm)			
	Group-I	Group-II	p-value*
Thickness of epidermis Extending from the surface of epidermis upto the dermal papilla	32.418±17.09	16.642±5.03	0.0016
Thickness of epidermis Extending from the surface of epidermis upto the epidermal ridges	165.5267±37.73	54.6±22.79	<0.0001
Thickness of dermis	2394.6±874.13	566.67±242.23	0.0088

[Table/Fig-5]: Data for thickness of epidermis and dermis (in μm) in both groups (p-value <0.05 considered significant).

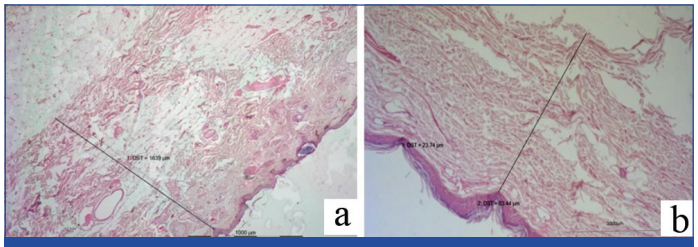

[Table/Fig-6]: Human skin tissue showing the thickness of dermis among both groups: Group-I and Group-II in (a,b), respectively (H&E stain, original magnification-10X with scale bar 400 μm).

In the young age group (Group-I), sebaceous glands depicted strong H&E staining along with well-defined nuclei [Table/Fig-7a]. However, in Group-II, the architecture of sebaceous glands was distorted, and the nuclei of cells showed pyknotic changes, as indicated by very light staining of nuclei and cells. Therefore, homogenisation of glandular tissue was seen in the advanced age group, i.e., Group-II, as shown in [Table/Fig-7b].

Picrosirius staining: Collagen fibres were found to be uniformly distributed and arranged in bundles, mostly lying parallel to the epidermis in both layers of the dermis in Group-I. Thick bundles of collagen fibres mostly showed red birefringence under a polarised microscope, indicating the presence of uniformly distributed Type-I collagen fibres in Group-I [Table/Fig-8a]. However, in Group-II, discrete and disorganised collagen fibres were more evident [Table/Fig-8b]. Collagen fibres appeared fragmented and were lying individually

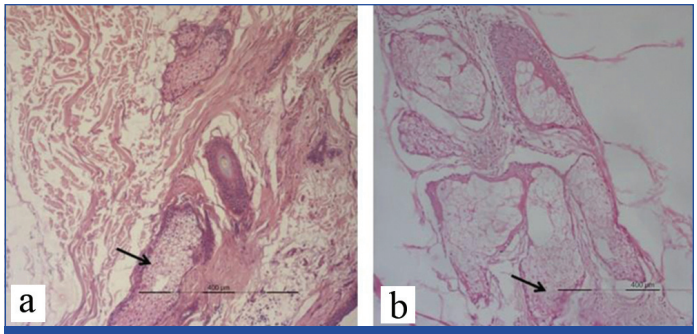

[Table/Fig-7]: Figure showing age-related changes in distribution of sebaceous glands among Group-I and Group-II in (a,b), respectively (H&E stain, original magnification 40X with scale bar 100 μm).

and far apart. The dermis showed mainly areas of disorganised collagen fibres in the papillary layer. Additionally, in Group-II, extensive homogenisation and light staining of collagen fibres were observed due to the disintegration of fibres. These disintegrated collagen fibres showed greenish-yellow birefringence under a polarised microscope, indicating a marked decrease in Type-I collagen fibres and an abundance of Type-II and Type-III collagen fibres. Furthermore, in Group-II, in most cases, there was separation between the dermis and epidermis due to the increase in the interfascicular space between collagen fibres of the papillary dermis in older individuals.

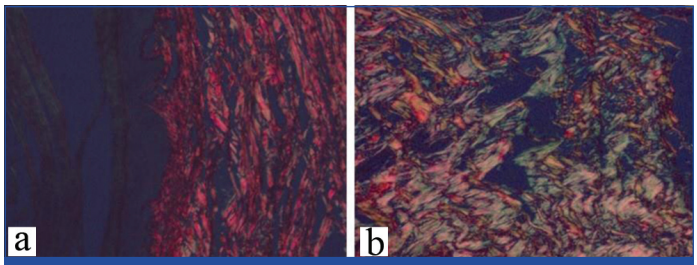

[Table/Fig-8]: Figure showing differential distribution of collagen fibers in both groups: Group-I (a) and Group-II (b). Thick bundles of collagen fibers mostly showed red birefringence under polarised microscope in Group-I. In Group-II, disintegrated collagen fibers showed greenish-yellow birefringence under polarised microscope (Picrosirius red stain, under polarising microscope, original magnification 40X with scale bar 100 μm).

DISCUSSION

Aging is a natural process, and the skin serves as an ideal marker of the chronological ageing process. Being an exposed organ, the skin is susceptible to environmental damage, particularly from Ultraviolet (UV) rays, which play a significant role in extrinsic aging and photoaging [11-13].

By analysing human skin tissue using the validated senescence marker p16Ink4a expression, it was observed that the number of p16INK4a positive cells was significantly higher in elderly individuals compared to younger age groups. Epigenetic factors may contribute to the modification of chromatin structure and DNA accessibility, shaping the gene expression of keratinocytes at different age groups and allowing dynamic and coordinated expression changes to maintain a balance between keratinocyte self-renewal and differentiation processes [14]. This balance between proliferation and differentiation is tightly regulated to ensure the maintenance of the stem cell population and preserve epidermal homeostasis throughout life. In the current study, the authors observed that in the aged population, this homeostatic balance is disrupted, leading to the accumulation of senescent, non dividing cell populations in the skin tissue of older individuals. After confirming the presence of a predominantly senescent cell population in the older age group, the authors aimed to assess the extent of DNA damage within these senescent cells. Immunofluorescence staining with the γH2AX antibody revealed a significant accumulation of γH2AX positive keratinocytes in the epidermis of the elderly population, while the expression pattern of γH2AX was negative in the younger population. This finding suggests a transformation of keratinocytes

from actively dividing to non dividing senescent cells in the skin of the elderly population. The increased frequency of senescent cells in the aged population, along with fragmented DNA, may be responsible for altered regenerative potential and functional decline of the tissue, leading to various age-related skin disorders.

Furthermore, the increased expression of γH2AX in the stratum spinosum layer of the epidermis reflects the age-associated decline in proliferative capacity, resulting in diminished epidermal thickness. This may be the reason for the significant decrease in the thickness of the epidermis among the aged population compared to the younger population. The present study is consistent with previous studies that have reported a significant decrease in the thickness of the epidermis among the elderly population, along with flattening of the dermoepidermal junction [15-17]. These factors may contribute to the cutaneous atrophic changes observed in the elderly population [18-20].

To date, not much data has been reported on the relative distribution of dermal collagen fibres among various age groups. In the current study, the authors observed a significantly decreased dermal thickness in the older population. The changes visualised in aged skin can be attributed to alterations in the relative distribution and arrangement of dermal collagen fibres, leading to modifications in its biomechanical properties. Collagen serves as the building block of various tissues and the extracellular matrix in the body. Any adverse variations or changes in its structure can accelerate the aging process in adults, contributing to premature morbidity, disability, and/or mortality [21]. Recent research has revealed that the content and ratio of collagen Type-I and collagen Type-III can represent the occurrence and development of diseases [21]. Additionally, the relative change in the content of collagen Type-I and collagen Type-III with increasing age also affects various skin properties, such as strength and elasticity [22-23].

In the current study, collagen fibres in the young population were found to be uniformly distributed and arranged parallel to the epidermis in the dermis, while in the elderly population, discrete disorganisation and fragmentation of collagen fibres were observed. Picrosirius staining showed a predominance of Type-I collagen fibres in the young population, whereas predominantly Type-II and Type-III collagen fibres were observed in the older population. Overall, the distribution of Type-I/Type-III collagen fibres was found to decrease in skin tissue with advancing age. Gao J et al., also reported similar findings, with a marked decrease in Type-I collagen and an increase in Type-III collagen fibres in skin samples from the elderly population [22]. Studies by Brown SR et al., and Liu JC et al., also demonstrated a decreased ratio of Type-I/Type-III collagen in aging skin tissue [23,24]. These observations suggest that age-related damage to the skin may mediate reduced cell-cell cohesiveness and decreased efficiency of the re-epithelialisation process. Furthermore, the authors of the current study observed a significant distortion in the architecture of sebaceous glands in the older population.

Limitation(s)

One of the limitations of the current study was that the functional role of both markers, γH2AX and p16INK4a, could not be studied as the present study was conducted on cadaveric tissues. Therefore, further work needs to be carried out to investigate the functional role of γH2AX and p16INK4a in the aging of skin tissue, as well as to evaluate potential therapeutics that can be used to treat age-related diseases.

CONCLUSION(S)

The present study has presented comprehensive data confirming the positive role of P16INK4a in aging skin tissue. A markedly significant difference was observed in the expression pattern of P16INK4a between the young and elderly populations. Furthermore, the DNA damage marker γH2AX showed positivity only in the older age group, further confirming the association between senescence and DNA damage. With advancing age, various significant changes were observed in the skin microstructure, such as a significant decrease in the thickness of the epidermis, flattening of the dermoepidermal junction, and a decreased ratio of Type-I/Type-III collagen fibres. Based on these findings, it can be inferred that the collagen synthetic capacity is low in aged individuals, leading to decreased repair and regenerative capacity. The current data on age-related DNA damage and resulting cellular senescence can provide the basis for age-related modifications of matrix proteins and play a crucial role in chronological aging and associated physiopathology.

Acknowledgement

The authors are thankful to Mr. Kaluram (Museum curator) and Ms. Jyoti (technician) for their contributions to the present study.

Acknowledging donor cadavers: The authors sincerely thank those who donated their bodies to the Department of Anatomy, enabling anatomical research to be conducted. The results from such research can potentially increase mankind's overall knowledge, which can then improve patient care. Therefore, these donors and their families deserve authors highest gratitude [25].

Authors' contributions: GR - Protocol development, data collection and analysis, manuscript writing; AA - Protocol development, data analysis, manuscript editing; GT - Manuscript editing; KC - Data collection, manuscript editing. All the authors approved the final draft of the paper.

REFERENCES

[1] Tripathi U, Misra A, Tchkonia T, Kirkland JL. Impact of senescent cell subtypes on tissue dysfunction and repair: Importance and research questions. Mech Ageing Dev. 2021;198:111548.
[2] Wiley CD, Campisi J. The metabolic roots of senescence: Mechanisms and opportunities for intervention. Nat Metab. 2021;(10):1290-301.
[3] Gorgoulis V, Adams PD, Alimonti A, Bennett DC, Bischof O, Bishop C, et al. Cellular senescence: Defining a path forward. Cell. 2019;179(4):813-27.
[4] Campisi J, Kapahi P, Lithgow GJ, Melov S, Newman JC, Verdin E. From discoveries in ageing research to therapeutics for healthy ageing. Nature. 2019;571(7764):183-92.
[5] Wagner KD, Wagner N. The senescence markers p16INK4A, p14ARF/p19ARF, and p21 in organ development and homeostasis. Cells. 2022;11(12):1966.
[6] Gasek NS, Kuchel GA, Kirkland JL, Xu M. Strategies for targeting senescent cells in human disease. Nat Aging. 2021;1(10):870-79.
[7] Patil P, Dong Q, Wang D, Chang J, Wiley C, Demaria M, et al. Systemic clearance of p16INK4a-positive senescent cells mitigates age-associated intervertebral disc degeneration. Aging Cell. 2019;18(3):e12927.
[8] Lee Y, Wang Q, Shuryak I, Brenner DJ, Turner HC. Development of a high-throughput γ-H2AX assay based on imaging flow cytometry. Radiat Oncol. 2019;14(1):150.
[9] Sedelnikova OA, Pilch DR, Redon C, Bonner WM. Histone H2AX in DNA damage and repair. Cancer Biol Ther. 2003;2(3):233-35.
[10] Goulding H, Pinder S, Cannon P, Pearson D, Nicholson R, Snead D, et al. A new immunohistochemical antibody for the assessment of estrogen receptor status on routine formalin-fixed tissue samples. Hum Pathol. 1995;26(3):291-94.
[11] Pagani EA, Jesus AM, Pereira GC, Neves RG, Nascimento LV. Envelhecimento cutâneo: Estudo comparativo clínico, histopatológico e histoquímico de áreas expostas e não expostas à luz solar. An Bras Dermatol. 1998;73(6):523-32.
[12] Landau M. Exogenous factors in skin aging. Curr Probl Dermatol. 2007;35:01-03.
[13] Hendi A, Wada DA, Jacobs MA, Crook JE, Kortuem KR, Weed BR, et al. Melanocytes in nonlesional sun-exposed skin: A multicenter comparative study. J Am Acad Dermatol. 2011;65(6):1186-93.
[14] Grönniger E, Weber B, Heil O, Peters N, Stäb F, Wenck H, et al. Aging and chronic sun exposure cause distinct epigenetic changes in human skin. PLoS Genet. 2010;6(5):e1000971.
[15] Lynch B, Pageon H, Le Blay H, Brizion S, Bastien P, Bornschlögl T, et al. A mechanistic view on the aging humanskin through ex vivo layer-by-layer analysis of mechanics and microstructure of facial and mammary dermis. Sci Rep. 2022;12(1):849.
[16] Pittayapruek P, Meephansan J, Prapapan O, Komine M, Ohtsuki M. Role of matrix metalloproteinases in photoaging and photocarcinogenesis. Int J Mol Sci. 2016;17(6):868.
[17] Oriá RB, Ferreira FV, Santana ÉN, Fernandes MR, Brito GA. Estudo das alterações relacionadas com a idade na pele humana, utilizando métodos de histo-morfometria e autofluorescência. An Bras Dermatol. 2003;78(4):425-34.
[18] Yaar M, Gilchrest BA. Skin aging: Postulated mechanisms and consequent changes in structure and function. Clin Geriatr Med. 2001;17(4):617-30.
[19] Fisher GJ, Kang S, Varani J, Bata-Csorgo Z, Wan Y, Datta S, et al. Mechanisms of photoaging and chronological skin aging. Arch Dermatol. 2002;138(11):1462-70.

[20] Rittie L, Farr EA, Orringer JS, Voorhees JJ, Fisher GJ. Reduced cell cohesiveness of outgrowths from eccrine sweat glands delays wound closure in elderly skin. Aging Cell. 2016;15(5):842-52.
[21] Roman RO, Kenny RA, Ross MM. Collagens and elastin genetic variations and their potential role in aging related diseases and longevity in humans. Exp Gerontol. 2020;129:01-12.
[22] Gao J, Guo Z, Zhang Y, Liu Y, Xing F, Wang J, et al. Age-related changes in the ratio of Type-I/III collagen and fibril diameter in mouse skin. Regen Biomater. 2023;10:rbac110.
[23] Brown SR, Cleveland EM, Deeken CR, Huitron SS, Aluka KJ, Davis KG. Type-I/Type-III collagen ratio associated with diverticulitis of the colon in young patients. J Surg Res. 2017;207:229-34
[24] Liu JC, Zhou L, Wang F, Cheng ZQ, Rong C. Osthole decreases collagen I/III contents and their ratio in TGF-b1-overexpressed mouse cardiac fibroblasts through regulating the TGF-b/smad signaling pathway. Chin J Net Med. 2018;16(5):321-29.
[25] Iwanaga J, Singh V, Ohtsuka A, Hwang Y, Kim HJ, Moryś J, et al. Acknowledging the use of human cadaveric tissues in research papers: Recommendations from anatomical journal editors. Clin Anat. 2021;34(1):02-04.

PARTICULARS OF CONTRIBUTORS:
1. Assistant Professor, Department of Anatomy, PGIMER, Chandigarh, India.
2. Professor and Head, Department of Anatomy, PGIMER, Chandigarh, India.
3. Associate Professor, Department of Anatomy, PGIMER, Chandigarh, India.
4. Associate Professor, Department of Anatomy, PGIMER, Chandigarh, India.

NAME, ADDRESS, E-MAIL ID OF THE CORRESPONDING AUTHOR:
Dr. Anjali Aggarwal,
Professor and Head, Department of Anatomy, PGIMER,
Chandigarh-160012, Punjab, India.
E-mail: anjli_doc@yahoo.com

PLAGIARISM CHECKING METHODS: [Jain H et al.]
- Plagiarism X-checker: Apr 10, 2023
- Manual Googling: Sep 01, 2023
- iThenticate Software: Sep 04, 2023 (11%)

ETYMOLOGY: Author Origin

EMENDATIONS: 6

AUTHOR DECLARATION:
- Financial or Other Competing Interests: None
- Was Ethics Committee Approval obtained for this study? No
- Was informed consent obtained from the subjects involved in the study? No
- For any images presented appropriate consent has been obtained from the subjects. NA

Date of Submission: **Apr 07, 2023**
Date of Peer Review: **Jun 20, 2023**
Date of Acceptance: **Sep 06, 2023**
Date of Publishing: **Oct 01, 2023**